

Supporting Information

Catalytic Deoxygenation of Stearic Acid into Olefins over Pt Catalysts Supported on MOF-derived Metal Oxides

Kok Bing Tan,^{a,c‡} Yiping Liu,^{a,c‡} Youting Wang,^{a,c} Sajid Ali,^{a,c} Wendong Wang,^{a,c} Jingru Li,^a Longmei Shang,^{a,c} Xing Yan,^a Xiaodong Zhang,^{b,*} and Guowu Zhan^{a,c*}*

^a Academy of Advanced Carbon Conversion Technology, College of Chemical Engineering, Integrated Nanocatalysts Institute (INCI), Huaqiao University, 668 Jimei Avenue, Xiamen, Fujian, 361021, P. R. China

^b College of Marine Equipment and Mechanical Engineering, Jimei University, 185 Yinjiang Road, Xiamen, 361021, Fujian, China

^c Fujian Provincial Key Laboratory of Biomass Low-Carbon Conversion, Huaqiao University, 668 Jimei Avenue, Xiamen, Fujian, 361021, P. R. China

**Corresponding author email: gwzhan@hqu.edu.cn (G. Zhan), shanglm@hqu.edu.cn (L. Shang) and xd_zhang77@aliyun.com (X. Zhang)*

‡ These two authors contributed equally to this work.

Number of pages: 9

Number of figures: 6

Number of tables: 1

Supplementary Figures

Figure S1. N ₂ physisorption isotherms of (a) ZrO ₂ , Pt/ZrO ₂ , and (b) Fe ₂ O ₃ samples.....	3
Figure S2. Thermogravimetric analysis (TGA) for UIO-66, Ce-BTC, and MIL-88B(Fe) metal-organic framework.	4
Figure S3. TEM image of (a) Pt/CeO ₂ , and (b) Pt/ZrO ₂ . Inset of (a, b) show the histogram of the particle size distribution of Pt nanoparticles.....	5
Figure S4. XPS data for Pt/ZrO ₂ in different regions: (a) Zr 3 <i>d</i> and (b) Pt 4 <i>f</i>	6
Figure S5. XPS data for Pt/Fe ₂ O ₃ in different regions: (a) Fe 2 <i>p</i> , (b) Fe 3 <i>p</i> , and (c) Pt 4 <i>f</i>	7
Figure S6. (a) TEM images of Pt/CeO ₂ before reaction, (b-c) EDX elemental maps of Pt/CeO ₂ before reaction, (d) TEM images of Pt/CeO ₂ after reaction, and (e-f) EDX elemental maps of Pt/CeO ₂ after reaction.....	8

Supplementary Table

Table S1. BET-specific surface area, pore diameter, and Pt loading amount of various samples.....	S9
--	----

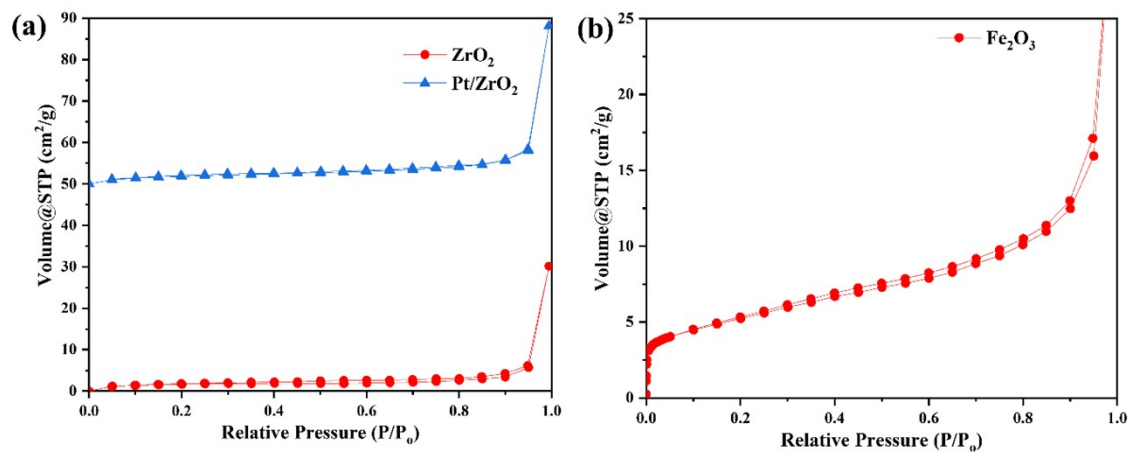


Figure S1. N₂ physisorption isotherms of (a) ZrO₂, Pt/ZrO₂, and (b) Fe₂O₃ samples.

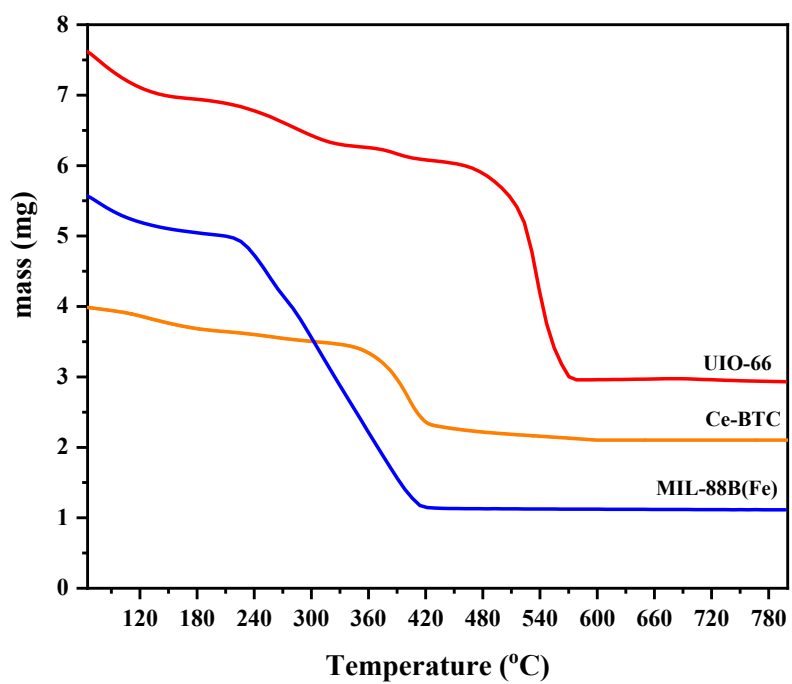


Figure S2. Thermogravimetric analysis (TGA) for UIO-66, Ce-BTC, and MIL-88B(Fe) metal-organic framework.

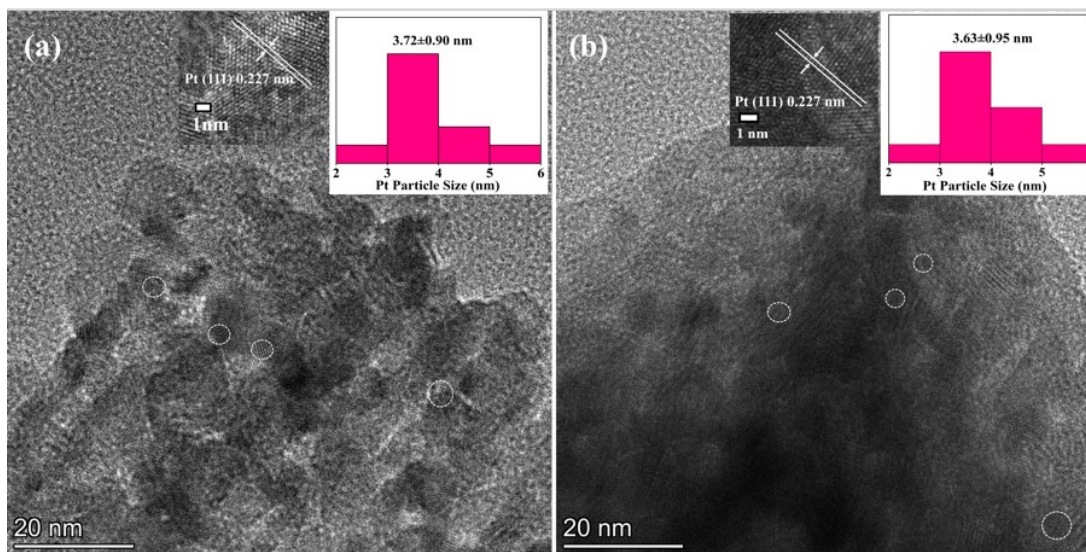


Figure S3. TEM image of (a) Pt/CeO₂, and (b) Pt/ZrO₂. Inset of (a, b) show the histogram of the particle size distribution of Pt nanoparticles

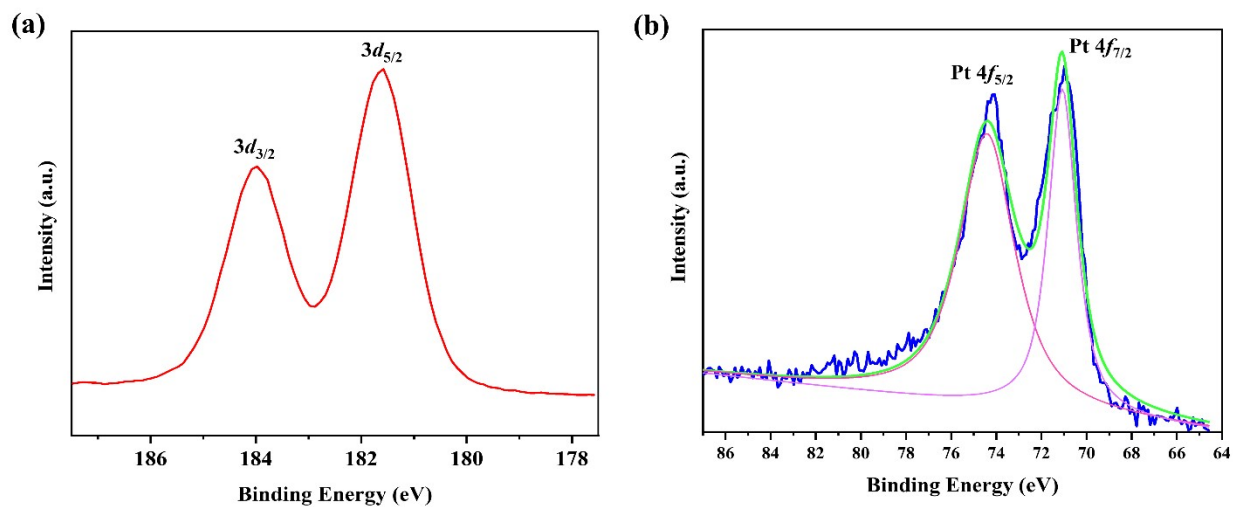


Figure S4. XPS data for Pt/ZrO₂ in different regions: (a) Zr 3d and (b) Pt 4f.

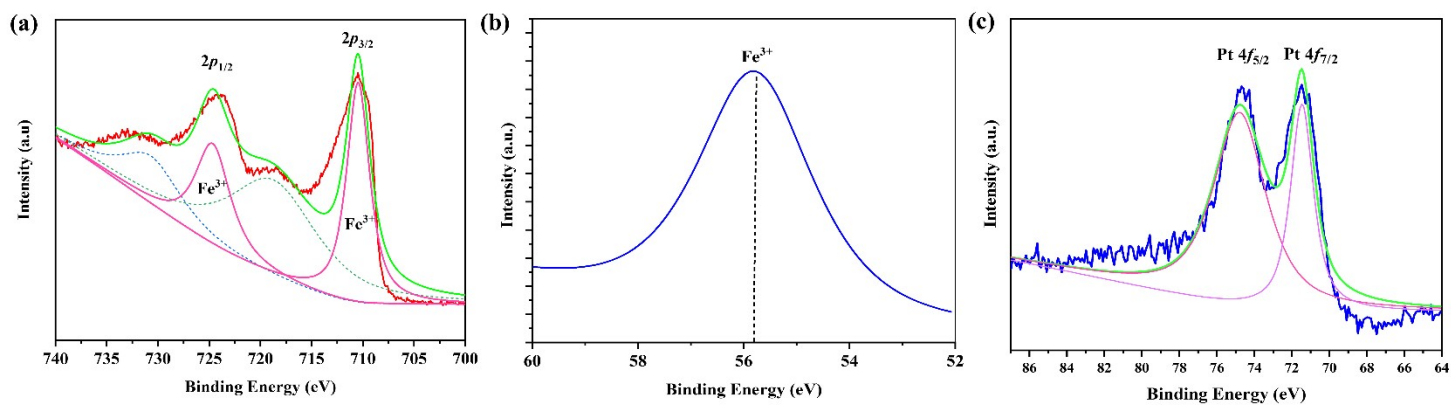


Figure S5. XPS data for Pt/Fe₂O₃ in different regions: (a) Fe 2p, (b) Fe 3p, and (c) Pt 4f.

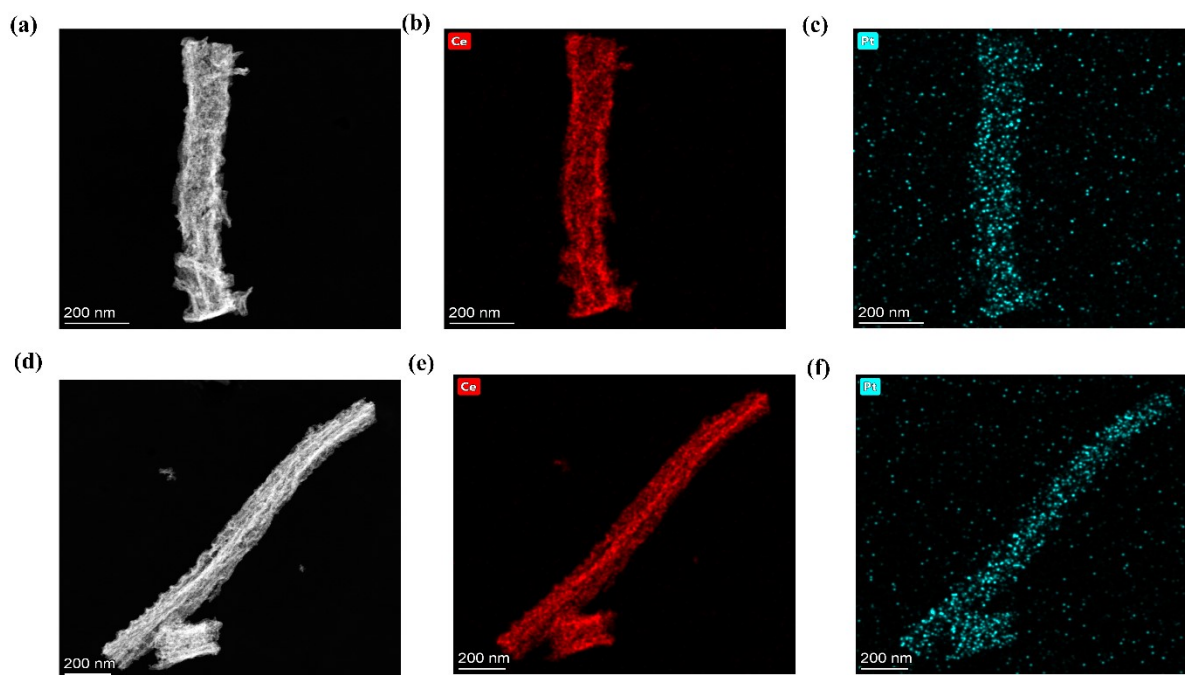


Figure S6. (a) TEM images of Pt/CeO₂ before reaction, (b-c) EDX elemental maps of Pt/CeO₂ before reaction, (d) TEM images of Pt/CeO₂ after reaction, and (e-f) EDX elemental maps of Pt/CeO₂ after reaction.

Table S1. BET-specific surface area, pore diameter, and Pt loading amount of various samples.

Sample	BET Surface area (m ² /g)	Pore diameter (nm)	pore volume (cm ³ /g)	Pt wt% ^a
Ce-BTC	21.1	4.5	0.09	-
CeO ₂	59.5	6.54	0.19	-
Pt/CeO ₂	53	3.41	0.15	3.2
UIO-66	1456	0.78	0.58	-
ZrO ₂	6.1	4.9	0.05	-
Pt/ZrO ₂	7.1	3.82	0.06	1.4
MIL-88(B) Fe	42.7	4.6	0.17	-
Fe ₂ O ₃	18.6	3.46	0.04	-
Pt/Fe ₂ O ₃	25	3.06	0.22	2.6

Note: ^a detected based on ICP- OES.